DOI: https://doi.org/10.15407/rpra30.01.065
UDC 621.375.4
PACS number: 07.57.-c

I.K. Kuzmychov [1], O.S. Lukash[1], O.B. Senkevych[1], O.V. Gribovsky [2]

[1] O.Ya. Usikov Institute for Radiophysics and Electronics NAS of Ukraine
12, Acad. Proskury St., Kharkiv, 61085, Ukraine
[2] Institute of Radio Astronomy of the NAS of Ukraine
4, Mystetstv St., Kharkiv, 61002, Ukraine
E-mail: kuzmichev.igr@gmail.com

SURFACE OSCILLATIONS IN OPEN RESONATORS WITH CURVILINEAR REFLECTORS

Subject and Purpose. *The subject of the work is the behavior of "bouncing ball" oscillations and surface oscillations in open resonant systems with curvilinear reflectors embedded in the waveguide transmission line. We seek to determine physical patterns and features of the interaction between volume "bouncing ball" oscillations and surface oscillations in open resonant systems with curvilinear reflectors.*

Methods and Methodology. *Basic quasi-optical techniques were employed. The electric field structures of considered oscillation types were measured using the probe-induced perturbation method. The resonant transmission coefficients of the open oscillating systems and the physical phenomena within them were experimentally studied with the aid of well-known microwave measurement techniques.*

Results. *A hemispherical open resonator (OR) and a mirror-lens resonator (MLR) have been studied to find that surface oscillations in both resonators are excited on the curvilinear surfaces of the reflectors and interact with the "bouncing ball" oscillations under certain conditions. In the hemispherical OR, this interaction occurs when $a/2w_1 = 0.927$, where a is the radius of the curvilinear reflector aperture and w_1 is the radius of the fundamental mode field spot on this reflector. In the MLR, the interaction between the fundamental mode oscillation and the surface oscillation localized on the lens surface is observed when $a_1/2w_1 = 1.351$.*

Conclusions. *The condition of small diffraction loss in the OR is known to be $a/2w_1 \geq 1$, and the possibility of the excitation of surface oscillations in the OR must always be considered because surface oscillations may mislead the researcher when examining solid dielectric specimens for the electrophysical parameters using the OR method. Thus, it is advisable to hold $L/R \leq 0.73$ in the hemispherical OR case and $L/F \leq 0.65$ in the MLR case.*

Keywords: *open resonator, mirror-lens resonator, surface oscillations, "bouncing ball" oscillations, resonant transmission coefficient, interaction of oscillations.*

Introduction

In the millimeter wave range, open resonators (ORs) of both hemispherical [1—5] and spherical geometries [1, 6, 7] are widely used to measure the electrophysical parameters of solid dielectrics. Certain objective reasons are behind this usage. First, being tens of the wavelengths in size, these open resonant systems are substantially larger than the millimeter-wave cavities and gain significantly in the loaded

Citation: Kuzmychov, I.K., Lukash, O.S., Senkevych, O.B., Gribovsky, O.V., 2025. Surface oscillations in open resonators with curvilinear reflectors. *Radio Phys. Radio Astron.*, **30**(1), pp. 65—73. https://doi.org/10.15407/rpra30.01.065

Q-factor due to a much larger volume occupied by the operating oscillation. Another advantage is the easy access to the resonant volume, with straightforward insertion of the measured specimen into the OR, or its effortless mounting on the OR mirror surface. Third, these resonant systems are free-space coupled, there is an additional angular selection of the excited oscillation spectrum. This is of particular value when identifying the operating oscillation in the OR loaded with a specimen to measure.

Typically, when measuring the electrophysical parameters of solid dielectrics in the OR, the fundamental TEM_{00q} mode is excited using concentrated coupling elements on the surface of the curvilinear reflector [1—7]. This scheme of the operating oscillation excitation in the resonator of hemispherical geometry is reasoned by the measured specimen location on the plane mirror surface [1—5]. The specimen does not need to be aligned perpendicular to the axis, which is the case in the resonator of spherical geometry. That is why the OR of hemispherical geometry is preferable.

There are practical cases when specimens are measured for the electrophysical parameters using a hemispherical OR with the normalized mirror spacing $L/R = 0.7$ to 0.9, where R is the curvature radius of the spherical mirror [5, 8, 9]. When L/R is within that range, the loaded Q-factor is at its maximum ($L/R = 0.7$ to 0.75, [10]). This is especially important when calculating the loss tangent of the measured specimen. At the same time, it was found [11, 12] that the resonant reflection and transmission coefficients suffer sharp changes when the mirror spacing of a hemispherical OR is in the range indicated. According to [13], in an OR with spherical mirrors, traditional "bouncing ball" oscillations [14] are excited alongside surface oscillations. These are localized near the curvilinear surface of the OR mirror and interact with the OR fundamental mode, yielding one degenerate oscillation. This decreases the loaded Q, changes the OR spectral characteristics [13], and as a result, affects the measured electrophysical parameters of the solid dielectrics. Therefore, in this work, we strive to experimentally detect surface oscillations in the OR with curvilinear reflectors and determine the physical patterns and features of the interaction between the surface oscillations and the "bouncing ball" oscillations.

1. Experimental setup

Figure 1 shows the block scheme of the cathetometer-based experimental setup. Its external view is seen in Fig. 2. The hemispherical OR is formed by spherical *1* and plane *2* mirrors with apertures $2a = 60$ mm. The curvature radius of the spherical mirror is $R = 113$ mm. The OR is fed by generator *4*, an extremely high frequency (EHF) source G4-142 for the frequency $f = 73.946$ GHz ($\lambda = 4.057$ mm). To expand the dynamic range during the measurements, the generator output signal is amplitude modulated by a meander (square wave) with a frequency of 1 kHz.

The signal enters the OR through slotted coupling element *9* like a rectangular waveguide taper from the standard 3.6×1.8 mm cross-section to the undersized one, 3.6×0.18 mm. Using coupling element *9*, the TEM_{00q} "bouncing ball" oscillation is excited in the OR.

The OR signal is output using slotted coupling element *19* like a rectangular waveguide taper from the undersized cross-section 3.6 × 0.16 mm in the center of plane mirror *2* to the main section of a 3.6×1.8 mm rectangular waveguide. The signal from generator *4* enters the waveguide transmission line through 3.6×2.0 mm dielectric (polyethylene) waveguide *6*. Two pyramidal horns *5* and *7* enhance the match of dielectric waveguide *6* with the generator and the waveguide transmission line. The horns are 19.5 mm long with 14.5×11.5 mm apertures. For additional decoupling of the OR from generator *4*, the scheme includes ferrite isolator *8* whose direct loss at 73.946 GHz frequency is –0.7 dB, while the reverse loss is –7.7 dB. The experimental setup also includes directional coupler *10* for monitoring the frequency of generator *4*. For this purpose, an additional waveguide transmission line is provided and includes measuring polarization attenuator *11*, resonant cavity wavemeter *12*, detector *13*, selective amplifier *14*, and oscilloscope *15* (see Figs. 1 and 2). The fourth arm of directional coupler *10* is connected with matched load *16*. Having passed through the OR, the signal enters the receiving path which includes measuring polarization attenuator *11*, detector *13*, selective amplifier *14*, and oscilloscope *15*.

To identify the oscillation types (modes) excited in the studied hemispherical OR, the probe-induced perturbation method is used [15]. The distribution of the electric component of the standing wave field

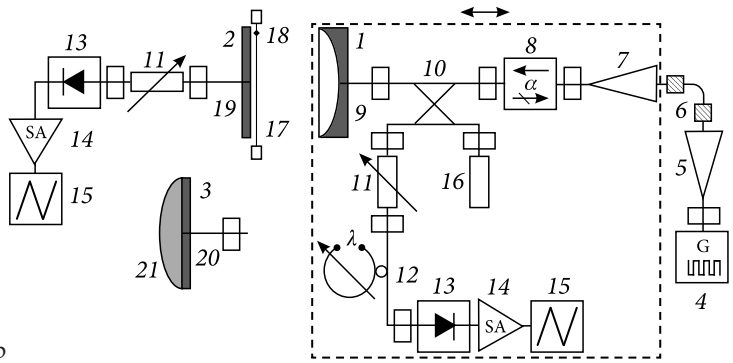

Fig. 1. Block-scheme of the experimental setup

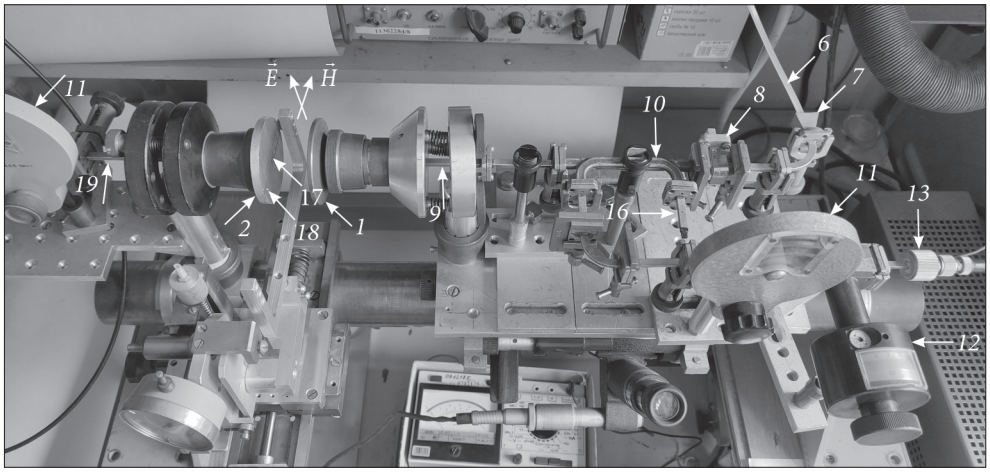

Fig. 2. External view of the waveguide part of the experimental setup

in the OR is measured using probe *18*. The probe looks like a glass ball with a diameter of 1 mm, coated with soot and fixed on 0.1 mm thick nylon thread *17* (Fig. 1). The probe moves in the $\vec{H}$ -plane of the TE_{10} waves inside slotted coupling elements *9* and *19* associated with the spherical and plane mirrors, respectively (Fig. 1). The OR oscillation structures are measured at the first anti-node of the electric field component of the OR standing wave, counting from the plane mirror.

The system is tuned to resonance by sliding the spherical mirror joined with a part of the waveguide path and accommodated on a movable platform. Just this part of the experimental setup is outlined with dashes in Fig. 1 and is viewed in the photo in Fig. 2. The OR mirror spacing is measured with an accuracy of ±0.001 mm.

The resonant transmission coefficient K_{transm} is determined using the following procedure [16]. After tuning the system to resonance via selective amplifier *14*, the signal level at the OR output is recorded via measuring polarization attenuator *11*. Denote it by N_1 (dB). After the measurement cycle has been completed, spherical mirror *1* and coupling element *9* are removed and replaced by the receiving path disconnected from the output of plane mirror *2* to be connected to the output of directional coupler *10*. The only thing is that the scheme additionally includes a phase shifter which is put before polarization attenuator *11* and helps achieve the maximum signal level by using the pointer device of selective amplifier *14*. The path attenuation is varied with the aid of measuring polarization attenuator *11*. Using selective amplifier *14*, we strive for the same signal level as in the K_{transm} measurements. Denote that signal level by N_2 (dB). Then the field resonant transmission coefficient is $K_{\text{transm}} = 10^{-\Delta N/20}$, where $\Delta N = N_2 - N_1$ (dB) [16].

2. Hemispherical OR. Measurement results

Figure 3 illustrates the resonant transmission coefficient K_{transm} measurement results versus the nor-

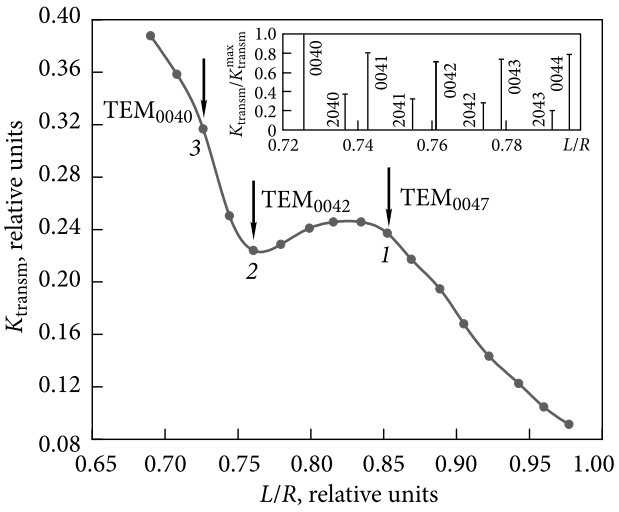

Fig. 3. The resonant transmission coefficient as a function of the mirror spacing for the OR fundamental mode

malized mirror spacing L/R for the fundamental "bouncing ball" TEM_{00q} oscillation in the examined hemispherical OR.

As the OR mirror spacing L/R diminishes, both ohmic and diffraction losses decrease. Consequently, the transmission coefficient K_{transm} for the fundamental TEM_{00q} oscillation increases. However, there is an exception in the range. Where the L/R space decreases from 0.835 (TEM_{0046}) to 0.726 (TEM_{0040}), the K_{transm} for the "bouncing ball" oscillation behaves anomalously and decreases. The same behavior of the resonance transmission coefficient K_{transm} was the case [11] for other OR geometries and in the presence of phase transparencies, such as strip diffraction gratings (both $\vec{H}$ - and $\vec{E}$ -polarizations) in the OR volume [17]. Such an L/R dependence of the K_{transm} might be attributed to the excitation of some oscillation alongside the TEM_{00q} mode with the following interaction between them. To verify this assumption, we analyzed the OR oscillation spectrum region in the L/R range, where the anomalous behavior of the resonant transmission coefficient K_{transm} is observed (Fig. 3).

From Fig. 3 it follows that as L/R in the studied OR decreases from 0.835 to 0.726, the fundamental TEM_{00q} oscillation is excited alongside the high axially asymmetric TEM_{20q} oscillation. Yet, it does not interact with the fundamental oscillation because of the separation by space. We work at a fixed frequency. The TEM_{20q} mode oscillation has a lower resonant transmission coefficient due to a larger diffraction loss. The TEM_{20q} and the fundamental TEM_{00q} belong to the same symmetry class [14] and can only interact when the OR is of semi-confocal geometry ($L/R \approx 0.5$). So, the TEM_{20q} oscillation does not interact with any "bouncing ball" oscillation excited in the OR under study, which is evident from Fig. 3. Paper [13] shows that the one to interact with a "bouncing ball" oscillation is a surface oscillation located on the curvilinear surface and excited due to the presence of the fundamental oscillation TEM_{00q} in the OR. The field energy of this oscillation is localized near the curvilinear surface of the spherical mirror. As the surface oscillation interacts with the OR fundamental oscillation, its field structure must change. This approach enables us to determine what plane on the spherical mirror surface localizes the energy of the surface oscillation field.

To check whether our reasoning is valid, let us analyze the electric field intensity distribution of the TEM_{00q} oscillation in the region of the K_{transm} anomalous behavior (Fig. 3). The electric component distribution in the OR standing wave field was measured by the probe-induced perturbation method, proceeding from the changes in the resonant transmission coefficient value [15]. We remind you that the absorbing probe diameter is $2d = 1$ mm, which comes from the condition $2d/\lambda \approx 0.23$ [18]. The distributions of the electric fields of the examined oscillation type in the two orthogonal planes correspond to the first antinode of the electric component of the OR standing wave field, counting from the plane mirror ($z \approx l/4$, with z being the coordinate on the OR axis).

Figure 4 shows the field amplitude distribution measured for several modes in the $\vec{H}$ -plane of the fundamental wave in the input waveguide. As seen, at $L/R = 0.853$ (TEM_{0047}, curve *1*) and $L/R = 0.726$ (TEM_{0040}, curve *2*), the considered modes have a Gaussian field distribution. Yet, the TEM_{0047} oscillation structure starts changing slightly near the OR axis. The calculated field distribution of the TEM_{0040} oscillation on the OR plane mirror is plotted (curve *3*) for comparison. This confirms the conclusion that the fields of the investigated "bouncing ball" oscillations in the OR obey the Gaussian distribution law.

In the $\vec{E}$ -plane of the TE_{10} wave in the input waveguide, the field structures of the studied TEM_{0047} and

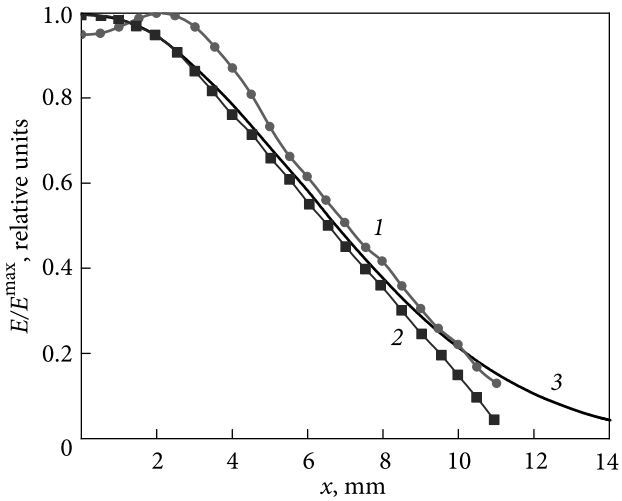

Fig. 4. Field structures of the studied oscillations in the $\vec{H}$ -plane: *1* — TEM_{0047}; *2* — TEM_{0040}; *3* — TEM_{0040}, the calculated field distribution

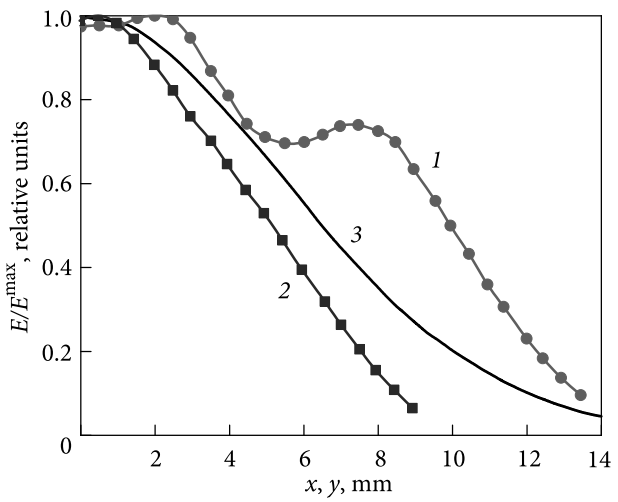

Fig. 5. The TEM_{0042} oscillation field structure: *1* — measured in the $\vec{H}$ -plane; *2* — measured in the $\vec{E}$ -plane; *3* — the calculated field distribution

TEM_{0040} modes look similar and represent circular Gaussian beams in the OR cross-section. The electrical field structure of the TEM_{0042} oscillation is different in kind ($L/R = 0.763$, Fig. 5). In the $\vec{H}$ -plane of the TE_{10} wave in the input waveguide, the electric field distribution of the studied oscillation (curve *1*, Fig. 5) becomes wider than the Gaussian field distribution (curve *3*, Fig. 5). In this case, the amplitude distribution of the oscillation field shows a series of positive and negative peaks. At the same time, in the $\vec{E}$ -plane, the field structure of the TEM_{0042} oscillation (curve *2*, Fig. 5) becomes narrower than the Gaussian distribution of the field at the L/R given (curve *2*).

The performed studies suggest that the TEM_{0042} mode oscillation interacts with the surface oscillation [13] whose field energy is localized like a narrow band in the $\vec{H}$ -plane on the OR spherical mirror. This has a devastating effect on the OR spectral characteristics, the K_{transm} decreases, and so does the loaded Q-factor. The radius of the TEM_{0042} mode field spot on the OR spherical mirror is [19]

$$w_1 = \sqrt{\frac{\lambda}{\pi} R \sqrt{\frac{L/R}{1 - L/R}}}. \qquad (1)$$

Substitute $\lambda = 4.057$ mm, $R = 113$ mm, and $L/R = 0.763$ into expression (1) and have $w_1 = 16.181$ mm. Then the spherical mirror radius $a = 30$ mm related to the diameter $2w_1$ of the TEM_{0042} mode field spot is 0.927.

The investigations carried out were the first to identify a surface oscillation in a hemispherical OR experimentally. The field energy of this oscillation is localized on the OR spherical mirror in the $\vec{H}$ -plane of the TE_{10} wave in the input waveguide. According to [10], the loaded Q-factor on the fundamental mode of a hemispherical OR is maximum when $L/R \le 0.75$. The surface oscillation interacts with the "bouncing ball" oscillation at approximately the same mirror spacing ($L/R = 0.763$).

We noted above that some authors measure the electrophysical parameters of solid dielectrics using a hemispherical OR with the mirror spacings as indicated. Therefore, care should be taken of the surface oscillation excitation possibility for the measuring cell when measuring the permittivity of solid dielectrics by the OR method. The existence of surface oscillations may be responsible for incorrect measurement results.

3. Mirror-lens OR. Measurement results

In the previous section, we showed that the surface oscillation can be excited on the curvilinear surface of one of the OR mirrors under certain conditions. Then the question arises as to whether or not oscillations of this type can exist on a convex surface in the axial excitation case. It is hardly reasonable to analyze resonators constituted by metal convex and plane mirrors, for resonators of this design are called

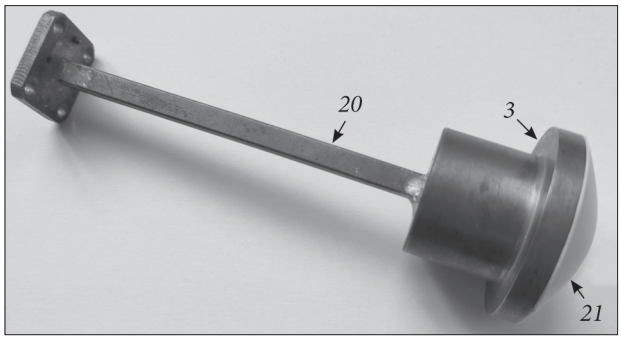

Fig. 6. The plane mirror with a dielectric lens

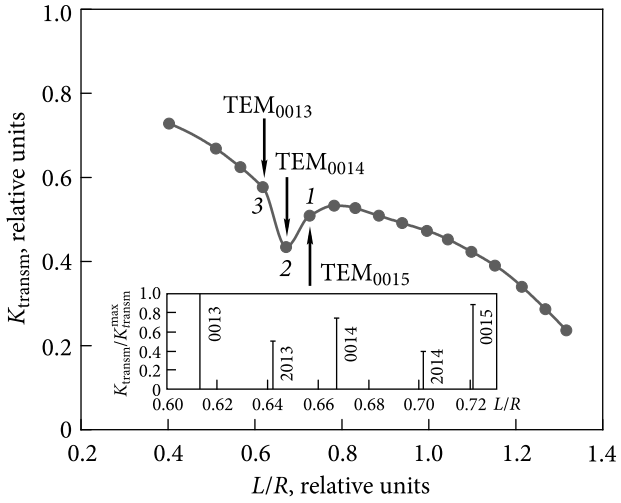

Fig. 7. The resonant transmission coefficient as a function of the MLR mirror spacing

unstable [19]. If so, let us consider an OR whose spherical mirror with curvature radius R is replaced by the system of a plane mirror and a plano-convex dielectric lens (see Figs. 1 and 6). The focal length of this lens is F. Its surface shape is a hyperboloid of rotation. In both resonators, the focusing properties of the phase corrector are identical for $R = F$ [19, 20].

Let us analyze the possibility of the surface oscillation excitation in a mirror-lens resonator (MLR). As previously, the experimental studies were conducted in the millimeter wave range. The block scheme of the experimental setup is as that in Fig. 1. The only difference is that spherical mirror *1* and coupling element *9* (Fig. 1) are replaced by plane mirror *3* combined with plano-convex lens *21* and coupling element *20* (Fig. 6). The lens material is fluoroplastic with dielectric constant $\varepsilon' = 2.08$. The focal length of the lens is $F = 39$ mm. The apertures of both plane mirrors in the OR are $2a_1 = 38$ mm. The MLR is excited through slotted coupling element *20* with its size of 3.6×0.16 mm in the center of plane mirror *3* (Figs. 1 and 6). The coupling element represents a rectangular waveguide taper between the undersized 3.6×0.16 mm and standard 3.6×1.8 mm cross-sections. The signal from the resonator is output through slotted coupling element *19* in the center of plane mirror *2*.

Figure 7 plots the measurement results of the resonant transmission coefficient K_{transm} versus the mirror spacing L/F for the "bouncing ball" TEM$_{00q}$ mode in the MLR. As L/F decreases, the K_{transm} in the MLR behaves the same as in the hemispherical OR (Fig. 3).

In the given range of the MLR mirror spacing, the resonant transmission coefficient of the TEM$_{00q}$ mode increases everywhere but for the L/F values featured by the wave mode interaction. This K_{transm} behavior is attributed to the fact that as L/F varies, the field spot diameter on mirror *3* with the plano-convex lens decreases, and so does the loss in the lens material, which is a decisive factor in raising the resonance transmission coefficient in the MLR tuning range. When $L/R > 1$ in the hemispherical OR, oscillations are not excited (Fig. 3) because the diffraction loss sharply rises. When $L/F > 1$, the MLR with a dielectric lens has "allowed" oscillation zones (Fig. 7), which agrees well with the results in [21].

As seen in Fig. 7, the value of the resonant transmission coefficient drops at $L/F = 0.667$ (point *2*). The oscillation spectrum analysis was performed to reveal that the "bouncing ball" TEM$_{0014}$ oscillation alone exists at $L/F = 0.667$, which is exactly what is reported in Fig. 7. Shown are two oscillation types having different longitudinal indices and excited in the MLR. In the MLR, the same as in the previously considered hemispherical OR, a surface oscillation exists, which affects the K_{transm}. The only difference is that the surface oscillation is localized on the dielectric lens surface in the LMR. To understand the reasons for this K_{transm} behavior, the electric field amplitude distribution in the resonator should be measured at points *1*, *2*, and *3* (Fig. 7) corresponding to the TEM$_{0015}$ mode ($L/F = 0.721$, point *1*), the TEM$_{0014}$ mode ($L/F = 0.667$, point *2*), and the TEM$_{0013}$ mode ($L/F = 0.613$, point *3*).

The studies were conducted using the probe-induced perturbation method described in the previous section. As before, the measurements of the electric field component of the MLR standing wave were performed at the first anti-node, counting from the

plane mirror. Fig. 8 illustrates the electric field amplitude distributions of the TEM_{0015}, TEM_{0014}, and TEM_{0013} modes measured in the $\vec{E}$-plane of the TE_{10} wave in the input waveguide.

According to Fig. 8, as the point $L/F = 0.667$ is approached from the side of the large mirror spacings, the MLR fundamental mode starts changing, see curve 1 for the TEM_{0015} oscillation. After passing $L/F = 0.667$ and reaching $L/F = 0.613$, the pure TEM_{0013} oscillation (curve *2*) exists. The above-said is supported by the electric field distribution of the TEM_{0013} oscillation in the $\vec{H}$-plane (curve *3*) of the TE_{10} wave in the input waveguide.

For comparison with the same-size hemispherical OR ($R = F$), Fig. 8 plots also the calculation results of the amplitude distribution of the TEM_{0013} electric field ($L/F = 0.613$, curve *4*). The good agreement between the field structures in both resonators suggests that the fundamental mode in the MLR is a circular Gaussian beam, as in the hemispherical OR.

Figure 9 displays the electric field amplitude distributions of the TEM_{0014} mode ($L/F = 0.667$, the MLR) in the $\vec{E}$- (curve *1*) and $\vec{H}$- (curve *2*) planes of the TE_{10} wave in the input waveguide. These can be compared with the calculated distribution of the TEM_{0014} mode electric field ($L/F = 0.667$, curve *3*) in the hemispherical OR ($R = F$).

From Fig. 9 it follows that in the $\vec{E}$-plane, the studied mode field distribution (curve 1) is much wider than the Gaussian distribution (curve *3*) and exhibits positive and negative peaks. At the same time, in the $\vec{H}$-plane, the TEM_{0014} field structure (curve *2*) is narrower than the Gaussian distribution (curve *3*) for the given L/F. Hence, it is reasonably safe to say that the examined mode oscillation interacts with the surface oscillation whose field energy is localized like a narrow strip in the $\vec{E}$-plane on the dielectric lens surface. This is what the modulation of the electric field amplitude distribution of the considered mode in the given plane tells. As in the hemispherical OR case, this degrades the MLR spectral characteristics and reduces the resonant transmission coefficient. The same as for the hemispherical OR, we determine the field spot radius w_1 of the TEM_{0014} mode on the lens-carrying mirror using expression (1). We take $R = F = 39$ mm, $L/F = 0.667$, and $\lambda_\delta = \lambda/\sqrt{\varepsilon'} = 4.057/\sqrt{2.08} = 2.813$ mm. Substituting them into expression (1) gives $w_1 = 7.03$ mm. The ratio of the mirror radius $a_1 = 19$ mm to the field spot diameter $2w_1$ results in a value of 1.351 for this MLR.

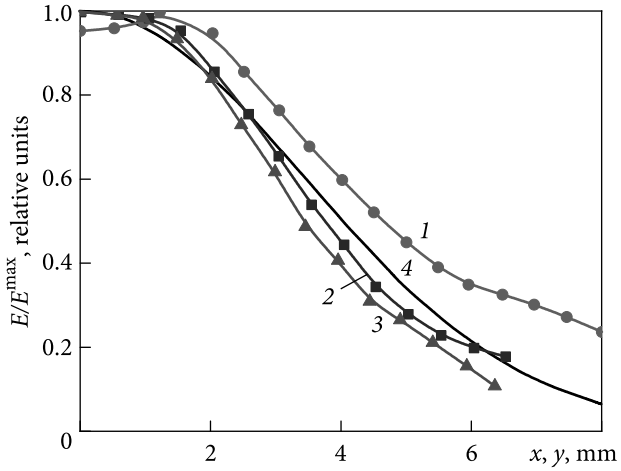

Fig. 8. Field structures of the TEM_{0015} and TEM_{0013} oscillations in the MLR: *1* — TEM_{0015} oscillation in the $\vec{E}$-plane; *2* — TEM_{0013} oscillation in the $\vec{E}$-plane; *3* — TEM_{0013} oscillation in the $\vec{H}$-plane; *4* — the calculated TEM_{0013} field distribution

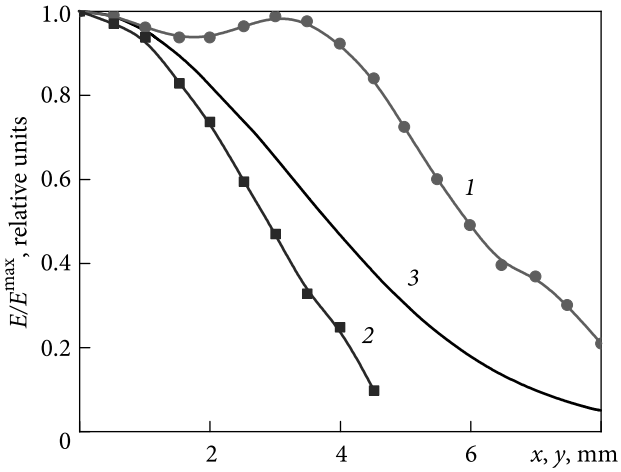

Fig. 9. The TEM_{0014} oscillation field structure in the MLR: *1* — in the $\vec{E}$-plane; *2* — in the $\vec{H}$-plane; *3* — the calculated TEM_{0014} field distribution

Thus, the performed study has shown that in a resonator with a dielectric lens, a surface oscillation is excited alongside the TEM_{0014} mode at $L/F = 0.667$. This oscillation is associated with the "bouncing ball" oscillation and has a devastating effect on the spectral characteristics of this electrodynamic system. This oscillation exists on the lens surface and is oriented in the $\vec{E}$-plane of the fundamental wave in the input waveguide. Therefore, in the MLR, a modified TEM_{0014} oscillation exists (Fig. 9). As shown in the

previous section, the surface oscillation in the hemispherical OR is oriented in the $\vec{H}$-plane of the fundamental wave in the input waveguide. The difference in the orientation of the surface oscillation on the exteriors of the phase correctors of the considered resonators can be attributed to the cumbersome MLR alignment and the presence of the dielectric lens itself in the resonator volume.

Conclusions

The experimental studies presented in this work suggest some important practical conclusions.

1. Based on the analysis of the fundamental TEM_{00q} oscillation behavior in the hemispherical OR with the mirror spacing varied, a surface oscillation has been identified. Its field energy is localized on the concave surface of the spherical mirror in the $\vec{H}$-plane of the TE_{10} wave in the input waveguide.

2. At a certain mirror spacing (specifically, at $L/R = 0.726$ to 0.835), the surface oscillation interacts with the "bouncing ball" oscillation because it belongs to the same symmetry class. This point should be considered properly when measuring the electrophysical parameters of solid dielectrics using the OR method. Such measurements in the indicated range of the OR mirror spacing are not unusual in the literature.

3. In the MLR, a surface oscillation is also excited and gets coupled to the TEM_{00q} oscillation of the resonator. This affects the MLR spectral characteristics. The field energy of the surface oscillation is localized like a narrow strip on the convex surface of the dielectric lens. In this case, the oscillation is oriented on the convex surface of the dielectric lens in the $\vec{E}$-plane of the TE_{10} wave in the input waveguide. In the MLR, the excitation of the surface oscillation is observed at the mirror spacing $L/F = 0.65$ to 0.75.

4. According to work [22], the condition of low diffraction loss in the OR case is determined by the inequality $a/2w_1 \geq 1$. In the hemispherical OR, the surface oscillation interacts with the fundamental mode when $a/2w_1 = 0.927$. In the MLR, the interaction of the "bouncing ball" oscillation with the surface oscillation localized on the lens surface occurs at $a_1/2w_1 = 1.351$. As one can see, the surface oscillation interacts with the TEM_{00q} oscillation in the case of small diffraction loss in the resonator. Therefore, the measurements used to determine the electrophysical parameters of solid dielectrics by the OR method must fit $L/R \leq 0.73$ in the hemispherical OR case and $L/F \leq 0.65$ in the MLR case.

REFERENCES

1. Karpisz, T., Salski, B., Koput, P., Krupka, J., and Wojciechowski, M., 2022. Measurement of Uniaxially Anisotropic Dielectrics with a Fabry–Perot Open Resonator in the 20—50 GHz Range. *IEEE Microw. Wirel. Compon. Lett.*, **32**(5), pp. 441—443. DOI: 10.1109/LMWC.2022.3155938
2. Krupka, J., 2021. Microwave Measurements of Electromagnetic Properties of Materials. *Materials*, **16**(17), pp. 1—21. DOI: 10.3390/ma14175097
3. Elwood, B.D., Grimes, P.K., Kovaca, J., Eibena, M., and Meinersa, G., 2024. Fabry–Perot open resonant cavities for measuring the dielectric parameters of mm-wave optical materials. *ArXiv:2411.01058v1 [physics.optics]*, pp. 1—12. DOI: 10.48550/arXiv.2411.01058
4. Rahman, R., Taylor, P.C., and Scales, J.A., 2013. A System for Measuring Complex Dielectric Properties of Thin Films at Submillimeter Wavelengths Using an Open Hemispherical Cavity and a Vector Network Analyzer. *Rev. Sci. Instrum.*, **84**(8), pp. 083901 (1—10). DOI: 10.1063/1.4816828
5. Breslavets, A.A., Rong, L., Gang, Z., Voitovich, O.A., Shubny, O.I., Glamazdin, V.V., Natarov, M.P., Rudnev, G.O., Eremenko, Z.E., Prokopenko, A.A., 2022. Hemispherical *X* Band Microwave Small-Sized Open Resonator for a Wide Range from 1 to 20 Permittivity Characterization of Solid-State Dielectrics. *Low Temp. Phys.*, **48**(1), pp. 43—50. DOI: 10.1063/10.0008963
6. Karpisz, T., Salski, B., Kopyt, P., and Krupka, J., 2019. Measurement of Dielectrics from 20 to 50 GHz with a Fabry–Pérot Open Resonator. *IEEE Trans. MTT.*, **67**(5), pp. 1901—1908. DOI: 10.1109/TMTT.2019.2905549
7. Kayro, N.S., Teterina, D.D., Badin, A.V., and Bilinskii, K.V., 2021. Automated system based on an open resonator for measuring the electrophysical parameters of sheet dielectrics. *J. Phys.: Conf. Ser.*, **1989**(1), pp. 012020 (1—5). DOI: 10.1088/1742-6596/1989/1/012020
8. Choi, J.J., and Seo, W.B., 2001. Measurements of Dielectric Properties at Ka-Band Using a Fabry-Perot Hemispherical Open Resonator. *Int. J. Infrared Milli.*, **22**(12), pp. 1837—1851. DOI: 10.1023/A:1015083819566
9. Dudorov, S.N., Lioubtchenko, D.V., Mallat, J.A., and Räisänen, A.V., 2005. Differential Open Resonator Method for Permittivity Measurements of Thin Dielectric Film on Substrate. *IEEE Trans. Instrum. Meas.*, **54**(5), pp. 1916—1920. DOI: 10.1109/TIM.2005.853352

10. Soohoo, R.F., 1963. Nonconfocal multimode resonators for masers. *Proc. IEEE*, **51**(1), pp. 70—75. DOI: 10.1109/PROC.1963.1661
11. Androsov, V.P., and Kuz'michev, I.K., 1987. Influence on the efficiency of excitation of the open resonator of its parameters and connection with the waveguide. *Kharkiv, Institute for Radiophysics and Electronics of AS USSR, Preprint*. No. 354, 28 p.
12. Kuz'michev, I.K., 1998. Experimental detection and analysis of the morse critical point of open electrodynamical structure involved in diffraction radiation oscillator. In: *Third Int. Kharkov Symp. "Physics and Engineering of Millimeter and Submillimeter Waves" (MSMW'98)*: proc. Kharkiv, Ukraine, 15—17 Sept. 1998, **1**, pp. 227—229. DOI: 10.1109/MSMW.1998.758 963
13. Svishchev, Yu.V., Tuchkin, Yu.A., and Shestopalov, V.P., 1990. Resonance mode tuning in an open resonator with spherical mirrors. *Reports of the USSR Academy of Sciences*, **312**(5), pp. 1111—1114.
14. Shestopalov, V.P., 1992. *Morse critical points of dispersion equations*. Kyiv, Ukraine: Naukova Dumka Publ., pp. 42—52.
15. Valitov, R.A. ed., 1969. *Submillimeter Wave Technique*. Moskow, USSR: Sovetskoe radio Publ., pp. 219–229.
16. Frait, Z., and Patton, C.E., 1980. Simple Analytic Method for Microwave Cavity Q Determination. *Rev. Sci. Instrum*., **51**(8), pp. 1092—1094. DOI: 10.1063/1.1136368
17. Kuzmichev, I.K., 1997. An efficient method of controlling the coupling between waveguide and open resonator. *Telecommunications and Radio Engineering*, **51**(11—12), pp. 113—118.
18. Vertiy, A.A., and Leonov, Yu.I., 1976. Study of the influence of probe dimensions on the nature of measured field distributions in open resonant systems. *Izv. vuzov. Radioelektronika*, **199**(2), pp. 105—107.
19. Tarasov, L.V., 1981. *Physics of processes in coherent optical radiation generators*. Moskow, USSR: Radio i Svyaz' Publ., pp. 197—212.
20. Kuzmichev, I.K., 1995. Mirror-lens open resonator. In: *Propagation of radio waves in the millimeter and submillimeter ranges*. Kharkiv, Ukraine: IRE of NAS Ukraine, pp. 121—131.
21. Androsov, V.P., Veliev, E.I., and Vertii, A.A., 1983. Polarization and spectral characteristics of open resonators with internal inhomogeneities. *Radiophys. Quantum Electron*., **26**(3), pp. 234—242. DOI: 10.1007/BF01045099
22. Gloge, D., 1964. General method for calculating optical resonators and periodic lens systems. In: *Proc. Quasi-Optics Symposium*. New York, USA, 8—10 June 1964. Moskow, USSR: Mir Publ., pp. 280—314.

Received 14.11.2024

І.К. Кузьмичов[1], О.С. Лукаш[1], О.Б. Сенкевич[1], О.В. Грибовський[2]

[1] Інститут радіофізики та електроніки ім. О.Я. Усикова НАН України
вул. Акад. Проскури, 12, м. Харків, 61085, Україна
[2] Радіоастрономічний інститут НАН України
вул. Мистецтв, 4, м. Харків, 61002, Україна

ПОВЕРХНЕВІ КОЛИВАННЯ У ВІДКРИТИХ РЕЗОНАТОРАХ З КРИВОЛІНІЙНИМИ ВІДБИВАЧАМИ

Предмет і мета роботи. Предметом роботи є поведінка коливання типу «стрибаючий м'ячик» та поверхневих коливань у відкритих резонансних системах з криволінійними відбивачами, які включені у хвилевідну лінію передачі. Метою роботи є встановлення фізичних особливостей і закономірностей взаємодії об'ємних коливань типу «стрибаючий м'ячик» та поверхневих коливань у відкритих резонансних системах з криволінійними відбивачами.

Методи та методологія. Для вирішення поставлених у роботі завдань використано основні методи квазіоптики: для вимірювання структур електричних полів розглянутих типів коливань було застосовано метод пробного тіла; в експериментальних дослідженнях резонансних коефіцієнтів передачі відкритих коливальних систем і фізичних явищ, що в них відбуваються, використовувалися добре відомі методи НВЧ-вимірювань.

Результати. У роботі розглянуто напівсферичний відкритий резонатор (ВР) та дзеркально-лінзовий резонатор (ДЛР). Виявлено, що на криволінійних поверхнях відбивачів обох типів резонаторів можуть збуджуватися поверхневі коливання, які за певних умов взаємодіють із коливанням резонатора «стрибаючий м'ячик». У напівсферичному ВР ця взаємодія має місце за умови $a/2w_1 = 0.927$ (a — радіус апертури криволінійного відбивача, w_1 — радіус плями поля основного типу коливань на цьому відбивачі). У ДЛР взаємодія основного типу коливань з поверхневим коливанням, локалізованим на поверхні лінзи, відбувається при $a_1/2w_1 = 1.351$.

Висновок. Відомо, що умови малості дифракційних втрат для ВР визначаються умовою $a/2w_1 \geq 1$. З огляду на це необхідно враховувати можливість збудження в резонаторі поверхневих коливань, які здатні призвести до невірних результатів при вимірюванні методом ВР електрофізичних параметрів твердих діелектриків. Тому дослідження доцільно проводити при $L/R \leq 0.73$ у разі застосування ВР напівсферичної геометрії. Якщо ж використовується ДЛР, то зразки бажано досліджувати за умови $L/F \leq 0.65$.

Ключові слова: *відкритий резонатор, дзеркально-лінзовий резонатор, поверхневі коливання, коливання «стрибаючий м'ячик», резонансний коефіцієнт передачі, взаємодія коливань.*